JOURNAL
OF THE AMERICAN CHEMICAL SOCIETY

VOLUME 94, NUMBER 8 APRIL 19, 1972

Conformational Analysis of Nucleosides in Solution by Quantitative Application of the Nuclear Overhauser Effect

Roger E. Schirmer, Jeffrey P. Davis,[1] Joseph H. Noggle, and Phillip A. Hart*[1]

Contribution from the Department of Chemistry and School of Pharmacy, University of Wisconsin, Madison, Wisconsin 53706. *Received July 9, 1971*

Abstract: The theory of the nuclear Overhauser effect (NOE) in molecules with internal degrees of freedom is developed and then applied to determine the range of conformations available to 2′,3′-isopropylideneinosine and 2′,3′-isopropylideneuridine in dimethyl-d_6 sulfoxide. Both molecules are found to exist primarily in the syn conformation, but with some population in the anti conformation as well. These results are discussed with respect to previous experimental and theoretical studies of nucleoside conformation in solution.

Mononucleosides affect biological systems in diverse ways. Many mononucleosides have antibiotic properties,[2a] and adenosine is a potent inhibitor of platelet aggregation.[2b] The nucleoside monophosphate esters are precursors in nucleic acid biosynthesis.[3] The 3′,5′-cyclic monophosphate of adenosine (cyclic AMP) is a ubiquitous secondary hormonal messenger.[4] Because of the potential importance of molecular conformation in determining biological activity, the conformations of nucleosides and nucleotides have been actively studied over the past decade.[5] In spite of extensive work in this area, a great deal of uncertainty remains as to the conformation which these molecules assume in solution.

The basis for all studies of nucleoside and nucleotide conformation is provided by the X-ray analysis of their structures, which provides accurate bond angles and bond lengths, and thus accurately determines the conformations present in the solid state. The solid-state conformations represent minima in the sum of intramolecular and intermolecular free energy in the crystal. While it is generally assumed that the intramolecular component of the free energy of a small molecule as a function of its conformation is very similar in the solid and liquid states, the intermolecular components may be very different, so that the lowest energy conformations in the crystal need not be identical with the lowest energy conformations in solution. In addition, it is usual to observe only one, or at most two, nucleoside conformations in the crystal.[6] From such information no conclusions can be drawn about the relative energies of the myriad other conformations which must be populated to some extent in solution. The X-ray data, which have been reviewed to 1969,[6,7] are nonetheless essential in interpreting data obtained by other means in terms of nucleoside conformation in solution.

The problem of the conformation of nucleosides in solution has usually been divided into two parts, the first part being the determination of the dihedral angles between the substituents (usually hydrogen) on the sugar and the second being the establishment of the relative orientation of the base and the sugar about the glycosyl bond. Elucidation of the sugar conformation has been approached primarily by analysis of the nmr coupling constants,[8] which indicate the deviation of ring atoms from a five-atom plane and give some information on the composition of the population of rotamers about the C4′–C5′ bond. The sugar conformation has been thought to have only minor effects on the orientation about the glycosyl bond in solution.

The conformational distribution about the glycosyl bond has not been so easily determined. The problem

(1) School of Pharmacy.
(2) (a) R. Suhadolnick, "Nucleoside Antibiotics," Wiley-Interscience, New York, N. Y., 1970; (b) G. V. R. Born, "Proceedings of the International Symposium on Pathogenesis and Treatment of Thromboembolic Diseases," Basel, 1966, p 159.
(3) J. N. Davidson, "The Biochemistry of the Nucleic Acids," 6th ed, Methuen, London, 1969.
(4) J. G. Hardman, G. A. Robison, and E. W. Sutherland, *Annu. Rev. Physiol.*, 33, 311 (1971), and references therein.
(5) R. U. Lemieux, *Can. J. Chem.*, 39, 116 (1961).
(6) M. Sundaralingam, *Biopolymers*, 7, 821 (1969).
(7) H. M. Sobell, "Genetic Organization," Vol. 1, Academic Press, New York, N. Y., 1969, p 91.
(8) D. B. Davies and S. S. Danyluk, *Can. J. Chem.*, 48, 3112 (1970), and references therein.

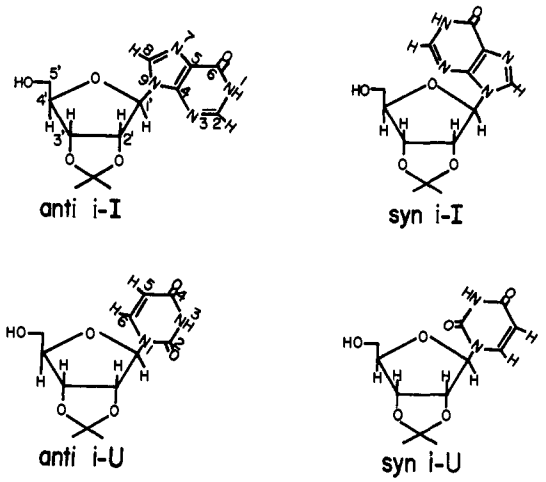

Figure 1. Structures of 2′,3′-isopropylideneinosine (i-I) and 2′,3′-isopropylideneuridene (i-U).

has been attacked by computation of steric barriers,[9,10] by steric–electronic calculations,[11] by nonbonded interaction computations,[12,13] by resonance energy computations,[14] by nmr coupling constant[15] and chemical shift analysis,[16] by infrared analysis of intramolecular hydrogen bonding,[17] by circular dichroism and optical rotatory dispersion,[18] and by qualitative application of the nuclear Overhauser effect both alone and correlated with circular dichroism.[19] Dipole moment measurements have been made on selected nucleosides, but the method has not been pursued.[20] A complete review of the analyses of nucleoside and nucleotide conformation in solution to 1968 is available.[21] Most workers in this area have interpreted their results in terms of a preferred anti conformation (see Figure 1 and the Appendix) about the glycosyl bond for both purine and pyrimidine nucleosides in solution. In all cases, however, it was necessary to reach conclusions indirectly by correlating the experimental results with data on model systems whose conformations were assumed known or by employing theories difficult to apply or incompletely developed. In order to resolve the uncertainties in these conclusions, an experimental method is required that has a sound theoretical foundation and that will yield general quantitative information on conformational distributions in solution.

(9) A. E. V. Haschemeyer and A. Rich, *J. Mol. Biol.*, 27, 369 (1967).
(10) A. V. Lakshminarayanan and V. Sasisekharan, *Biochim. Biophys. Acta*, 204, 49 (1970).
(11) I. Tinoco, R. C. Davis, and S. R. Jaskunas in "Molecular Associations in Biology," B. Pullman, Ed., Academic Press, New York, N. Y., 1968.
(12) A. V. Lakshminarayanan and V. Sasisekharan, *Biopolymers*, 8, 475 (1969).
(13) H. R. Wilson and A. Rahman, *J. Mol. Biol.*, 56, 129 (1971).
(14) F. Jordan and B. Pullman, *Theor. Chim. Acta*, 9, 242 (1968).
(15) R. J. Cushley, I. Wempen, and J. J. Fox, *J. Amer. Chem. Soc.*, 90, 709 (1968).
(16) M. P. Schweizer, J. T. Witowski, and R. K. Robins, *ibid.*, 93, 277 (1971), and references therein.
(17) J. Pitha, S. Chladek, and J. Smrt, *Collect. Czech. Chem. Commun.*, 28, 1622 (1963).
(18) (a) D. W. Miles, W. H. Inskeep, M. J. Winkley, R. K. Robins, and H. Eyring, *J. Amer. Chem. Soc.*, 92, 3872 (1970); (b) W. H. Inskeep, D. W. Miles, and H. Eyring, *ibid.*, 92, 3866 (1970).
(19) P. A. Hart and J. P. Davis, *ibid.*, 93, 753 (1971), and references therein.
(20) P. Mauret and J.-P. Fayet, *C. R. Acad. Sci., Ser. C*, 264, 2081 (1967).
(21) P. O. P. Ts'o in "Fine Structure of Proteins and Nucleic Acids," G. D. Fasman and S. N. Timasheff, Ed., Marcel Dekker, New York, N. Y., 1970, p 49.

The intramolecular proton nuclear Overhauser effect (NOE) provides a sensitive measure of relative internuclear distances and has been applied quantitatively to rigid systems.[22] We show in the present paper how the NOE can be quantitatively applied to the analysis of conformationally mobile systems in solution and use as examples a purine nucleoside, 2′,3′-isopropylideneinosine (i-I), and a pyrimidine nucleoside, 2′,3′-isopropylideneuridine (i-U). See Figure 1.

Theory

In this section the theory of the nuclear Overhauser effect in rigid molecules which we reported previously[22] will be extended to include nonrigid molecules. We will be primarily interested in the determination of the major conformations present when a range of conformational possibilities exists and when exchange between the various conformations is specifically allowed. The notation used will be that of Noggle and Schirmer,[23] which differs slightly from that of ref 22.

The nuclear Overhauser effect can be described quantitatively as the fractional enhancement of the resonance of spin d when the resonances of spins s are saturated, or

$$f_d(s) = \frac{\text{area of } d \text{ when } s \text{ is saturated} - \text{equilibrium area of } d}{\text{equilibrium area of } d} \quad (1)$$

An internal motion can be viewed as a movement of d along an appropriate path in a molecule-fixed coordinate system: the effect of the internal motion on $f_d(s)$ can then be determined by dividing the path into N segments and using McConnell's equation[24] to describe the behavior of the magnetization of d in each segment. The equation is

$$\frac{dM_{zd}(i)}{dt} = -R_d(i)[M_{zd} - M_{0d}] - \sum_n \sigma_{dn}(i)[M_{zn}(i) - M_{0n}(i)] + k_{i+1,i}M_{zd}(i+1) + k_{i-1,i}M_{zd}(i-1) - (k_{i,i+1} + k_{i,i-1})M_{zd}(i) \quad (2)$$

where $M_{zd}(i)$ is the z component of magnetization of spin d in conformation i, $M_{0n}(i)$ is the equilibrium value of $M_{zn}(i)$, and k_{ij} is the rate constant for the transfer of spins from the ith segment to the jth segment. $R_d(i)$ is the total spin–lattice relaxation rate of spin d when it is on the ith segment of its path and is given by

$$R_d(i) = \sum_{j \neq d} \rho_{dj}(i) + \rho_d^*(i) \quad (3)$$

In this equation, $\rho_{dj}(i)$ is the spin–lattice relaxation rate of spin d due to its dipole coupling with spin j. Such equations are applicable if the rate of exchange between segments is slower than the correlation time for relaxation. If the molecule is at sufficient dilution so that only intramolecular dipole coupling between d and j need be considered

$$\rho_{dj}(i) = \gamma_d^2\gamma_j^2\hbar^2\tau_c(dj)/r_{dj}^6 \quad (4)$$

(22) R. E. Schirmer, J. H. Noggle, J. P. Davis, and P. A. Hart, *J. Amer. Chem. Soc.*, 92, 3266 (1970).
(23) J. H. Noggle and R. E. Schirmer, "The Nuclear Overhauser Effect: Chemical Applications," Academic Press, New York, N. Y., 1971.
(24) H. M. McConnell, *J. Chem. Phys.*, 28, 430 (1958).

and, for homonuclear spins

$$2\sigma_{dj}(i) = \rho_{dj}(i)$$

where $\tau_C(dj)$ is the correlation time for the reorientation of the vector joining spins d and j and $r_{dj}(i)$ is the distance between d and j in conformation i. The term $\rho_d^*(i)$ in eq 3 includes the contributions to the relaxation of spin d from all mechanisms other than the intramolecular dipole–dipole mechanism. The other mechanisms may include spin rotation, anisotropic chemical shift, and quadrupole interactions as well as dipole–dipole interactions with solvent molecules, impurities, or dissolved oxygen (*cf.* ref 23).

The solution of the problem of internal motions can be divided into three regions on the basis of the rate of exchange:

Region I	Slow	$k \ll R_d$
Region II	Intermediate	$R_d \ll k \ll \tau_C^{-1}$
Region III	Fast	$k \gtrsim \tau_C^{-1}$

We will not be concerned with fast motions as eq 2 is not valid in region III and the theory of the effects of rapid internal motions has not been thoroughly investigated.[23] It might be noted at this point that the only other limitation on the validity of eq 2 that might be significant in the context of this paper is that the spin system must be loosely coupled.

Solution of Eq 2 in Region I. In this region the rate of exchange between conformations is slow compared to the relaxation rate of the spins (R_d) and so the exchange terms of eq 2 can be neglected. If spins s have been saturated for a sufficiently long time, a steady-state assumption can be made for *each* conformation and the NOE enhancements of the spins in conformation i are given by

$$f_d(s,i) = \frac{M_{zd}(i) - M_{0d}(i)}{M_{0d}(i)} = \sum_s \frac{\gamma_s}{2\gamma_d}\frac{\rho_{ds}(i)}{R_d(i)} - \sum_j \frac{\gamma_j}{2\gamma_d}\frac{\rho_{dj}(i)f_j(s,i)}{R_d(i)} \quad (5)$$

Since only a single spectrum will be observed for all of the conformations, the experimental NOE enhancement is

$$f_d(s) = \sum_i \chi_i f_d(s,i) \quad (6)$$

where χ_i is the fraction of molecules in conformation i. Equation 6 can be easily generalized to a continuous path described by internal variables Ω

$$f_d(s) = \frac{\int f_d(s,\Omega)P(\Omega)d\Omega}{\int P(\Omega)d\Omega} \quad (7)$$

where $P(\Omega)$ is the distribution function for the variable Ω.

Solution of Eq 2 in Region II. To compute the NOE when the internal motion falls into region II, we begin by summing eq 2 over all segments i to obtain

$$\sum_i R_d(i)[M_{zd}(i) - M_{0d}(i)] - \sum_i \sum_j \sigma_{dj}(i)[M_{zj}(i) - M_{0j}(i)] = 0 \quad (8)$$

where a steady-state assumption has been made so that the derivative is zero, and the exchange terms cancel identically since closure of the path requires $N + i = i$ so that

$$\sum_i k_{i,i+1}M_{zd}(i) = \sum_i k_{i-1,i}M_{zd}(i-1)$$

$$\sum_i k_{i,i-1}M_{zd}(i) = \sum_i k_{i+1,i}M_{zd}(i+1)$$

In order to solve eq 8 for $f_d(s)$, a relation between $M_{zd}(i)$, M_{zd}, and χ_i must be derived where $M_{zd} = \Sigma_i M_{zd}(i)$. This is done by noting that under steady-state conditions with $k \gg R_d$, eq 2 becomes

$$k_{i+1,i}M_{zd}(i+1) + k_{i-1,i}M_{zd}(i-1) - (k_{i,i+1} + k_{i,i-1})M_{zd}(i) = 0 \quad (9)$$

As the molecules will have their equilibrium distribution among the possible conformations, we can use the principle of microscopic reversibility to obtain

$$-(k_{i,i+1} + k_{i,i-1})\chi_i + k_{i+1,i}\chi_{i+1} + k_{i-1,i}\chi_{i-1} = 0 \quad (10)$$

Using eq 9 and 10 plus the two identities, $M_{zd} = \Sigma_i M_{zd}(i)$ and $1 = \Sigma_i \chi_i$, we obtain the required relation[23]

$$M_{zd}(i) = \chi_i M_{zd} \quad (11)$$

Substituting (11) into (8) and rearranging, we obtain

$$f_d(s) = \sum_s \frac{\gamma_d}{2\gamma_s}\frac{\langle\rho_{ds}\rangle}{\langle R_d\rangle} - \sum_j \frac{\gamma_d}{2\gamma_j}\langle\rho_{dj}\rangle f_j(s)/\langle R_d\rangle \quad (12)$$

where we have defined

$$\langle R_d\rangle = \sum R_d(i)\chi_i \text{ and } \langle\rho_{dj}\rangle = \sum_i \rho_{dj}(i)\chi_i$$

The generalization to a continuous path in this case involves only replacing the latter two definitions with

$$\langle R_d\rangle = \int R_d(\Omega)P(\Omega)d\Omega \Big/ \int P(\Omega)d\Omega$$

and

$$\langle\rho_{dj}\rangle = \int \rho_{dj}(\Omega)P(\Omega)d\Omega \Big/ \int P(\Omega)d\Omega \quad (13)$$

$P(\Omega)$ is again a distribution function of the internal variable Ω.

Comparing eq 12 with 7 we see that it is the ρ_{ij} which must be averaged in the intermediate rate region (region II), while it is the $f_i(j)$ which must be averaged in the slow-exchange region (region I). This difference is the result of the fact that when $k \ll R_d$, the molecule remains in each conformation long enough to come to a steady state so that the observed NOE is simply the ensemble average of the NOE's characteristic of each conformation. On the other hand, when $k \gg R_d$, the residence time of the molecule in each conformation is sufficiently short that all conformations will be sampled in the time it takes the system to reach a steady state, and thus the ensemble average interactions must be used to compute the NOE. The details of the procedures used to calculate enhancements from eq 7 and 12 are given in Appendix I.

Experimental Section

Sigma grade 2′,3′-isopropylideneinosine (i-I) and 2′,3′-isopropylideneuridine (i-U) were purchased from Sigma Chemical Co., St. Louis, Mo., and lyophilized from D_2O before use. Both i-I and i-U were made up as 0.25 M solutions in DMSO-d_6 (Stohler Isotope Chemicals, 99.5% D) in a coaxial assembly ("coax") as

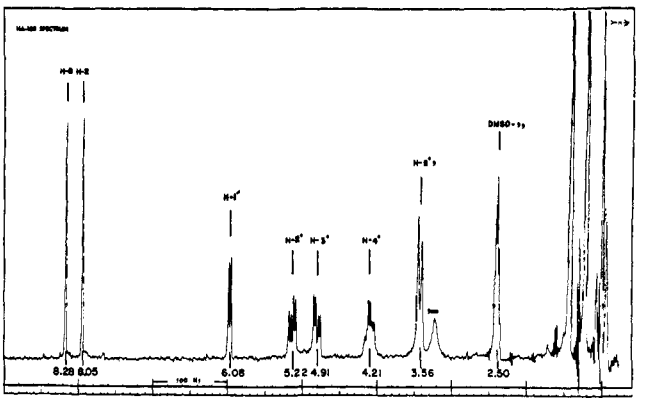

Figure 2. Nmr spectrum of i-I, 0.25 M in DMSO-d_6 plus 1.8% (v/v) *tert*-butyl-d_1 alcohol, 31.0°.

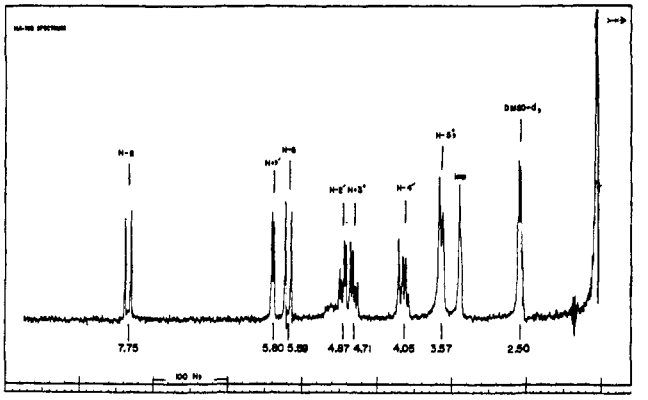

Figure 3. Nmr spectrum of i-U, 0.25 M in DMSO-d_6 plus 1.8% (v/v) *tert*-butyl-d_1 alcohol, 31.0°.

previously described.[22] Each was also made up as a 0.25 M solution in DMSO-d_6 containing 1.8% v/v *tert*-butyl alcohol (Merck Sharpe and Dohme, Ltd., 99% isotopic purity) ("standard tube"). The four samples were degassed by at least three freeze–pump–thaw cycles at less than 10^{-5} Torr before being sealed off.

We chose the isopropylidene derivatives as models on which to develop the quantitative application of the nuclear Overhauser effect to internally mobile systems because their simple nmr spectra are particularly amenable to a large number of double-resonance experiments, and because we were initially quite concerned about the possible effects of ribose conformational freedom on the glycosyl conformational fits. Dimethyl sulfoxide was used as the solvent for the nmr studies, since it is to our knowledge one of the very few available deuterated substances which is able to dissolve many typical nucleosides at concentrations which do not require time-averaged nmr experiments. The 100-MHz nmr spectra of the i-I and i-U NOE samples in standard tubes at 30° are given in Figures 2 and 3, with proton assignments and apparent chemical shifts. Chemical shifts quoted here were measured from the DMSO-d_5 resonance and converted to δ_{TMS} by addition of 2.50 ppm, the chemical shift of DMSO-d_5 from internal TMS. Quoted spin-coupling constants are apparent, *i.e.*, measured directly from the spectra without correcting for tight coupling.

Nuclear Overhauser effect experiments were done on a Varian HA-100 nmr spectrometer run in frequency sweep mode, with an observing field of 0.15 mG and a decoupling field of from 2.75 to 3.5 mG. Area-based NOE's were computed by averaging ten determinations made on a single day of ten interactions. For each interaction a reference trace and an Overhauser trace were taken alternately ten times. Each of the 20 traces made for each interaction was then integrated by planimeter twice and the result averaged. The ten computed area enhancements for the particular interaction were then averaged.

Table I. Nuclear Overhauser Effect Enhancements[a] for 0.25 M i-I in DMSO-d_6 at 30°

Proton obsd	Proton saturated H-1′	H-2′	H-3′	H-4′	H-5′	H-8	H-2
H-1′		0.02[b]	−0.03	0.09		0.16	0.0
H-2′	0.01[b]			−0.02		0.10	0.04
H-3′	−0.03			−0.04	0.10	0.01	0.03
H-4′	0.10						
H-8	0.18	0.14	0.04		0.04		
H-2	0.1	0.07	0.07		0.06		

[a] Selected numbers from this table were used in the conformational fittings of i-I (see below). [b] These numbers are questionable, since they had very large σ's (±0.08). They are also anomalously small; *cf.* Calculations and Results below. These are area-based NOE measurements.

Peak-height-based NOE's were measured as described in ref 19. At least 5 and in many cases [*e.g.*, $f_8(1')$, $f_8(2')$, $f_8(3')$] more than 15 peak-height-based measurements made on several different days were averaged to obtain the values reported in Table I. The maximum σ for any given experimental value is 0.03, *i.e.*, $f_{4'}(1') = 0.10 \pm 0.03$ and $f_8(3') = 0.04 \pm 0.03$. This points up the fact that the major limitation to this type of experiment is the present precision of commercial nmr spectrometers.

Area determinations were made on the standard tube i-I sample, and peak-height measurements were performed on this sample and on a 0.25 M coaxial sample with external lock. Data from the two types of samples were identical. The two types of measurements gave data that in all cases agreed within experimental error. The extreme disagreement is in the $f_8(1')$, $f_8(2')$, $f_8(3')$ experiments, which, on the basis of area measurements, are 0.16, 0.16, and 0.08, respectively. As a possible cause of these disagreements, the existence of H-8 spin coupling was investigated. Since we were not able to detect a change in the width of the H-8 resonance upon irradiation of H-1′, it seems unlikely that H-8 and H-1′ are J coupled. It is also unlikely that H-8 is J coupled to H-2′ or H-3′.

Because of the fact that the area-based experiments were performed on a single day and the peak-height values were accumulated on several different days and using two different samples, and because the area measurements seemed less reliable, the peak-height data (Table I) were used for conformational fittings. Using the same basic ribose geometry, computer fit of the ten area-based NOE enhancements resulted in a final two-Gaussian distribution nearly identical with that obtained from peak-height NOE's (*cf.* Calculations and Results below) except that the population in the anti range ($\Upsilon \approx 165°$) was increased from 23 to 29% of the total. Such a change is within the uncertainty of the experiment: changes of comparable magnitude can be caused by changes in other parameters.

All conceivable dipole–dipole relaxation pathways of the nucleoside protons were checked. Saturation of the DMSO-d_5 peak produced no enhancements of any of the other resonances in either the i-U or the i-I spectrum. Neither did saturation of the small impurity at about δ 3.50 produce any enhancements. Noise decoupling of the solvent deuterium spectrum in the i-I sample resulted in no measurable changes in intensity of the nucleoside resonances.

The experimental NOE's used for fitting a glycosyl conformation for i-U in DMSO have been revised slightly from those reported in ref 19. The conclusions reached there are not at all altered. The small changes are due to the averaging in of later experimental results.

Glycosyl Torsion Angle Conventions. We define here a new convention for specification of the nucleoside glycosyl torsion angle for two reasons. It is most consistent with modern terminology[25] and it simplifies computational procedures.

A purine nucleoside is taken to be syn when the C-8, X-8 bond is coplanar with the C-1′, X-1′ bond. The anti conformation is attained by rotation of the nucleobase by 180°. A pyrimidine nucleoside is taken to be syn when the C-5, C-6 bond is coplanar with the C-1′, X-1′ bond. The anti conformation is obtained from the syn conformation by rotating the nucleobase 180°. We use Υ to denote the glycosyl torsion angle and assign it a value of 0° when the nucleobase is in the extreme syn conformation. Υ is taken as the dihedral angle measured clockwise from the plane containing X-1′, C-1′ and the glycosyl bond to the plane of the

(25) W. Klyne and V. Prelog, *Experientia*, **16**, 521 (1960).

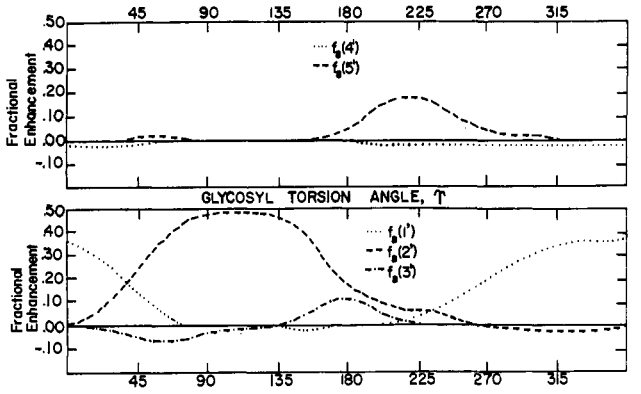

Figure 4. Plots of calculated intramolecular NOE's for i-I *vs.* glycosyl torsion angle. Calculations were done using geometry IIIA, $A = 0.0005$.

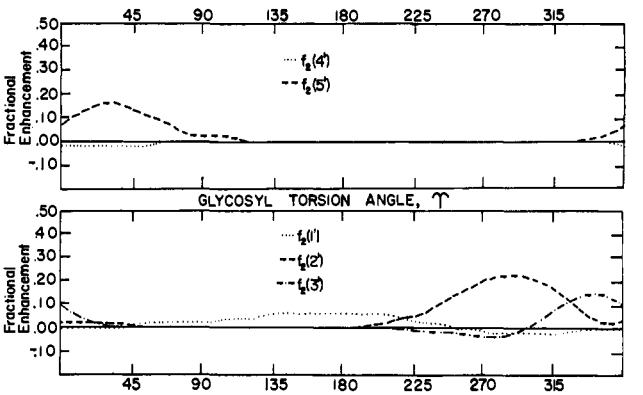

Figure 5. Plots of calculated intramolecular NOE's (see caption of Figure 4).

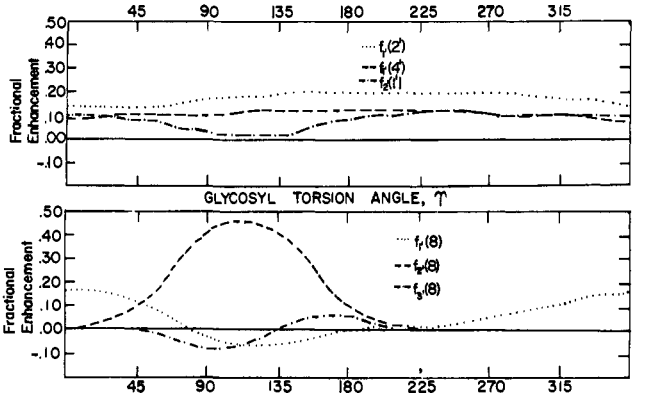

Figure 6. Plots of calculated intramolecular NOE's (see caption of Figure 4).

nucleobase when viewing down the glycosyl bond from the base to the sugar. Other glycosyl torsion angle conventions χ[6] and ϕ_{CN}[26] are related to Υ as

$$\Upsilon = (-\chi - 120°) \text{ modulus } 360°$$

$$\Upsilon = (\phi_{CN} - 120°) \text{ modulus } 360°$$

Framework Molecular Models, Prentice Hall, Englewood Cliffs, N. J., were used to construct nucleoside structures of i-I, based on the X-ray bond angles and lengths of adenosine in ref 27, and i-U, based on the X-ray of uridine 5′-monophosphate in ref 28.

CD measurements were made on a Cary 60 recording spectropolarimeter fitted with a Model 6002 CD attachment, with the slit programmed for a half-bandwidth of 1.5 nm. The low-wavelength region of the spectrum was inaccessible for the DMSO solutions because of high solvent absorbance below *ca.* 250 nm. The CD is recorded as molecular ellipticity, $[\theta]$, in units of degree square centimeter per decimal and absorbances never exceeded 2. The instrument was calibrated using (+)-camphorsulfonic acid (Aldrich).

Calculations and Results

Nucleoside conformation can be described by the torsion angle, Υ, about the glycosyl bond plus a set of parameters defining the ribose conformation. In this section, the results of extensive calculations of the NOE in 2′,3′-isopropylideneinosine (i-I) as a function of these parameters are presented and compared with experimental results. A more limited treatment of 2′,3′-isopropylideneuridine (i-U) will also be given.

Except as noted, the ribose geometries were based on standard bond lengths and angles: 109.5° for sp^3 carbons, 120° for ether oxygens, a C–H bond length of 1.0 Å, and other bond lengths as found in the appropriate X-ray crystal structure.[27,28] N-9 is trigonal and the C-5′–O-5′ bond is coplanar with the C-4′–H-4′ bond. The conformation was then specified in terms of the distance between H-1′ and H-4′ and the dihedral angles around the ribose ring. The four ribose conformations used in the study reported here are defined in Table II. See Appendix II.

The first step in the conformational analysis is to use eq 5 to calculate the various NOE enhancements as a function of Υ for the different ribose conformations and different choices of the relaxation parameter A. The enhancements calculated for i-I with ribose geometry IIIA and an external relaxation parameter of A = 0.0005 (see Appendix I) for all spins are shown in Figures 4, 5, and 6. All other reasonable ribose geometries give similar results, while increasing values of A cause a general decrease in the magnitude of the calculated NOE for any given value of Υ. For these and all calculations of this section, the protons were assumed to be loosely coupled; this approximation is not fully valid for H-2′ and H-3′ ($J_{2'3'}/\delta_{2'3'} \approx 0.19$) but should not introduce any large error into the results. The two C-5′ protons and the isopropylidene methyl protons were approximated as multiple spins located at their average position. These approxima-

Table II. Definition of Ribose Geometries Used in Fitting the NOE Data

	$r_{1'4'}$, Å	Dihedral angles, deg: H-1′–H-2′	H-2′–H-3′	H-3′–H-4′
Geometry I[a]	3.3	90	30	160
Geometry II[b]	3.0	115	0	115
Geometry IIIA[c]	3.0	95	30	170
Geometry IIIB	*d*	*d*	*d*	*d*

[a] C-3′ is approximately 0.3 Å endo. [b] Essentially a planar ribose with O-4′ 0.2 Å endo. The isopropylidene methyls were not included. [c] C-3′ is approximately 0.4 Å endo, all bond angles conventional. [d] Geometry IIIB is the same as IIIA except that the O-1′–C-1′–N-9 angle is 110°, the C-8–N-9–C-1′ angle is 128°, and the C-4–N-9–C-1′ angle is 127°. These angles correspond exactly with the angles found in adenosine by X-ray (see ref 2).

(26) J. Donohue and K. N. Trueblood, *J. Mol. Biol.*, 2, 363 (1960).
(27) A. E. V. Haschemeyer, and H. M. Sobell, *Acta Crystallogr.*, 18, 525 (1965).
(28) E. Shefter and K. N. Trueblood, *ibid.*, 18, 1067 (1965).

Table III. The Deviations of the Calculated NOE Enhancements from the Average Experimental Values for i-I[a]

Basic geometry		I	I	II	II	IIIA	IIIA	IIIA	IIIA	IIIB	IIIB
exchange region		II	II	II	II	II	II	I	II	II	I
$A \times 10^4$		5	5	5	5	5	5	5	0	5	5
i {j}[c]	$f_i(j)$[c]	1	2	3[b]	4[b]	5	6	7	8	9	10
8 {1′}	0.18	0.03	0.02	0.01	0.01	0.01	−0.01	−0.02	0	−0.01	−0.04
8 {2′}	0.14	−0.01	−0.01	−0.01	−0.02	0	−0.03	0.01	−0.01	−0.02	0.00
8 {3′}	0.04	0.02	0.04	0.02	0.03	0.02	0.06	0.03	0.01	0.03	0.03
8 {5′}[d]	0.04	0.04	0.04	0.04	0.04	0.03	0.03	0.03	0.02	0.04	0.03
1′ {8}	0.16	0.06	0.06	0.02	0.01	0.04	0.02	0.07	0.04	0	0.05
2′ {8}	0.10	0.04	0.04	0.03	0.02	0.04	0.02	0.02	0.04	0.01	−0.01
3′ {8}	0.01	0	0.01	0	0.01	0	0.02	0.01	0	0.01	0.00
2 {1′}	0.00	0	0	−0.01	0	−0.01	0	−0.02	−0.02	−0.01	−0.01
2 {2′}	0.07	0.07	0.07	−0.01	−0.01	0.02	0.03	0.03	−0.03	0.01	0.03
2 {3′}	0.07	0.01	0.01	−0.03	−0.04	−0.01	−0.02	0.03	−0.05	0.02	0.04
2 {5′}[e]	0.06	−0.02	−0.01	0.05	0.05	0.01	0.01	0.01	−0.03	0.04	0.04
1′ {2′}	0.02		−0.17		−0.11		−0.11				
2′ {1′}	0.01		−0.10		−0.06		−0.07				
1′ {4′}	0.09		0.04		0.01		0.00			0.01[e]	
Υ_1, deg		359	356	8	4	355	356	10	357	347	5
$\delta\Upsilon_1$, deg		8	6	93	84	64	51	110	77	46	92
w_1		0.83	0.93	0.76	0.83	0.80	0.71	0.78	0.76	0.84	0.59
Υ_2, deg		143	140	184	155	166	152	171	176	156	155
$\delta\Upsilon_2$, deg		9	3	7	6	10	5	7	8	4	4
σ		0.035	0.063	0.025	0.042	0.021	0.041	0.030	0.027	0.022	0.032

[a] Columns 1–10 list f(exptl) − f(calcd) for the various conditions indicated. [b] Isopropylidene methyl protons not included in these analyses. [c] i {j} notation indicates that j is saturated and the enhancement of i is recorded. $f_i(j)$ is the average experimental enhancement. [d] Calculated Overhauser effects due to saturation of the two 5′ protons were approximated. [e] Value calculated separately—not included in least-squares fit or σ.

tions do not have a strong effect on the conformational analysis because of the relatively remote position of the isopropylidene methyls and the limited use which is made of enhancements involving the 5′ protons; it should be kept in mind that the calculated enhancements involving the 5′ protons (see Figures 4 and 5) are subject to greater error than the others discussed here.

The enhancements of H-8 shown in Figure 4 follow the intuitively expected pattern as Υ is varied; the largest values of $f_8(i)$ occur when H-8 is near i. $f_8(4')$ is very small for all values of Υ because the H-8–H-4′ distance is relatively large; the slight negative values are due to the indirect polarization (a "three-spin" effect[23]) through H-5′ ($\Upsilon \sim 210$–$240°$) and H-1′ ($\Upsilon \sim 270$–$60°$). The smallness of the enhancements of the base protons when H-4′ is saturated is expected to hold in most nucleosides. This is fortuitous since, in many cases, the H-4′ nmr resonance overlaps that of another ribose proton so that saturating H-4′ may be unavoidable when saturating the other proton. The effects of such a coincidence can be seen to be minimal, but can be rigorously included in the calculations if one wishes to do so.

The enhancements of H-2 (Figure 5) show a similar pattern but with much smaller peak values because H-2 is, at all Υ, farther from the ribose protons than H-8 and thus is proportionately more sensitive to intermolecular relaxation (the enhancement can be approximated by $r_{mn}^{-6}/[A + \sum_j r_{mj}^{-6}]$; see Appendix I).

The calculated enhancements when H-2 is saturated (not shown) are very small at all Υ because the other spins are much closer to one another than they are to H-2. Because of this, the enhancements when H-2 was saturated were not used for the conformational analysis. It is important to note that in choosing which enhancements to use in determining the conformation, we do not necessarily choose those which are experimentally the largest, but rather those which vary the most with conformation. An enhancement of 0.02, while barely measurable, may be just as informative as an enhancement of 0.18 if it *could* be much different in certain conformations.

The intraribose enhancement $f_{1'}(4')$ (Figure 6) is not particularly sensitive to Υ, but was included in some of our analyses because it is quite sensitive to ribose geometry.

When the graphs of the enhancements *vs.* Υ are compared to the experimental values given in Table I, it appears that a single conformation cannot fully explain the results. Therefore, a two-Gaussian population distribution function was fit to the experimental data using the least-squares criterion for quality of fit (see Appendix I). A two-Gaussian function was selected because theoretical studies typically indicate two minima in the energy *vs.* Υ curve,[9,10,12–14] and because the NOE is much more sensitive to the gross features of the distribution than to exact local slopes and amplitudes so that any physically reasonable, convenient curve would be expected to reliably reproduce the main features of the actual distribution when it is fit to the NOE data. The distribution function will be discussed in terms of Υ_1 and Υ_2, the glycosyl torsion angles locating the centers of the two Gaussians; $\delta\Upsilon_1$ and $\delta\Upsilon_2$, the widths of the Gaussians at half-maximum height; and w_1 and w_2, where w_1 is the fraction of the area under the distribution function which is contributed by the major Gaussian and $w_1 + w_2 = 1$. If the two Gaussians do not overlap very much, w_1 and w_2 would be the fraction of the molecules in conformations centered about Υ_1 and Υ_2, respectively.

The distribution function was fit to the experimental data using several different ribose geometries (Table II), various values of A, and using programs written for both exchange rate regions I and II. The results of

several of these fits are presented in Table III. The standard deviations (σ) recorded in the table represent deviations of the final fit calculated enhancements from the mean experimental value. Comparing the σ values in the table with the standard deviation of the experimental enhancements about their own mean, which is about 0.02, shows that many of the fits recorded in Table III are very good indeed. The standard deviations for the fits given in columns 5 and 9, for example, have σ = 0.021 and 0.022, with none of the individual deviations exceeding 0.04.

Generally speaking, calculations using the equations for region II give slightly better fits (compare columns 5 with 7 and 9 with 10 in Table III) than those using the equations for region I. The differences are not large enough to eliminate region I from consideration, but it should be noted that region II covers rates of conformational exchange of approximately $1-10^8$ sec^{-1} and seems more likely than region I, which covers rates slower than 1 sec^{-1}. It was also found that an intermolecular contribution to the spin-lattice relaxation of A = 0.0005 worked slightly better than other values (*e.g.*, compare columns 8 and 9 in Table III), but with any value between A = 0.0 and 0.001 being satisfactory. This is a very reasonable range for intermolecular relaxation at room temperature in solutions of the composition used in these studies. In any case, the distribution function obtained was not very sensitive to the value of A or the rate region, so further discussion will be limited to calculations using the region II equations with A = 0.0005.

It should be noted that the A values quoted in this paper have units of $Å^{-6}$. A = 0.0005 is equivalent to the relaxation effect of a proton at 3.55 Å, since $(0.0005)^{-1/6} = 3.55$.

Several examples of distribution functions obtained using different ribose geometries are reproduced in Table III. It can be seen that the resulting distribution functions and σ values are not strongly dependent on small changes in the ribose conformation. More extensive studies indicate that any ribose geometry of i-I having an H-1′–H-4′ distance between 2.8 and 3.2 Å and any physically reasonable value (judging from the coupling constants) for the H-2′–H-3′ and H-1′–H-2′ dihedral angles, ranging from a planar ribose to C-3′ endo, appears to work equally well.

The H-1′–H-2′ enhancements (Table III, columns 2, 4, and 6) present some problem. Any reasonable ribose geometry makes the H-1′–H-2′ distance 2.8–3.2 Å, and it is difficult to explain the small experimental values of $f_{1'}(2') = 0.02$ and $f_{2'}(1') = 0.01$ when the spins are so close. It is unlikely that the low values are a result of the H-2′–H-3′ scalar coupling, since other enhancements involving H-2′ appear normal. One possibility would be if the interaction of the isopropylidene methyl with H-2′ were grossly underestimated and, at the same time, H-1′ and H-4′ were somewhat closer together than 2.9 Å. Note that the interaction of the isopropylidene methyl with H-2′ can be quite different from its interaction with H-3′ because the dioxolane ring is puckered.[29] Another possibility is rapid exchange among several conformations of the ribose and/or isopropylidene ring. There is no way of deciding among these and other possible explanations at the present time, but the distribution functions obtained when $f_{1'}(2)$, $f_{2'}(1')$, and $f_{1'}(4')$ are included in the fit are very similar to those obtained when they are discarded (compare columns 1 and 2, 3 and 4, and 5 and 6 in Table III), so the resolution of this inconsistency is not necessary to the conclusions of this paper.

The results presented up to this point indicate that the fits of glycosyl conformation are not highly sensitive to the ribose conformation, the value of A, or the exact rate of the internal rotation about the glycosyl bond. The calculations presented in Table IV show

Table IV. Calculated and Experimental NOE Enhancements for i-I

Parameters	1[a]	2	3[b]	4	5	6
Υ_1, deg	355	166	359	90	180	270
$\delta\Upsilon_1$, deg	64	64	88	92	92	92
Υ_2, deg	166	355				
$\delta\Upsilon_2$, deg	10	10				
w_2	0.20	0.20	0	0	0	0
Obsd {satd}	Exptl	Calcd enhancements[c]				
8 {1′}	0.18	0.17	0	0.21	0	−0.01	0.16
8 {2′}	0.14	0.14	0.40	0.16	0.46	0.40	0.05
8 {3′}	0.04	0.02	0	−0.04	−0.02	0	0.01
8 {5′}	0.04	0.01	0.01	0.01	0	0.02	0.07
1′ {8}	0.16	0.12	0	0.13	0	−0.04	0.07
2′ {8}	0.10	0.06	0.31	0.06	0.40	0.31	0.01
3′ {8}	0.01	0.01	0	−0.01	−0.06	−0.01	0
2 {1′}	0.00	0.01	0.04	0	0.03	0.05	0
2 {2′}	0.07	0.05	0.01	0.06	0	0.02	0.15
2 {3′}	0.07	0.08	0.04	0.07	0.01	0	0
2 {5′}	0.06	0.05	0.01	0.05	0.05	0	0.01
σ		0.021	0.13	0.032	0.16	0.14	0.12

[a] Best-fit two Gaussian. [b] Best-fit one Gaussian. [c] Calculations use the region II type averaging, A = 0.0005, and geometry IIIA.

that the enhancements *are very sensitive* to the conformational distribution function that we wish to determine. Column 1 of Table IV shows the enhancements calculated from the best two-Gaussian distribution function. In column 2, the enhancements are calculated with the positions of the two Gaussians exchanged; *i.e.*, the distribution function is rotated by ~180° so that the bulk of the population is in the anti conformation. As can be seen, the results of transposing the distributions are disastrous, particularly for $f_8(1')$, $f_8(2')$, $f_{1'}(8)$, and $f_{2'}(8)$. The standard deviation increases from 0.02 to 0.13.

Column 3 of Table IV gives the enhancements resulting from fitting a one-Gaussian (two-parameter) distribution function to the data. It can be seen that this works nearly as well as the two-Gaussian fit (five parameters) with only $f_8(3')$ being very far off. More important, the two-parameter fit has converged to the major population of the five-parameter function, but with the single Gaussian being characteristically somewhat broader than either of the two Gaussian peaks. Columns 4–6 of Table IV then show the enhancements calculated for a single 90° wide Gaussian in the other three quadrants. It is apparent that no conformation but syn can adequately explain the experimental results. It should be noted at this point that while we consider the positions of the peak populations, Υ_1 and Υ_2, to be quite reliable, the widths of the peaks, $\delta\Upsilon_1$ and

(29) J. Zussman, *Acta Crystallogr.*, 6, 504 (1953).

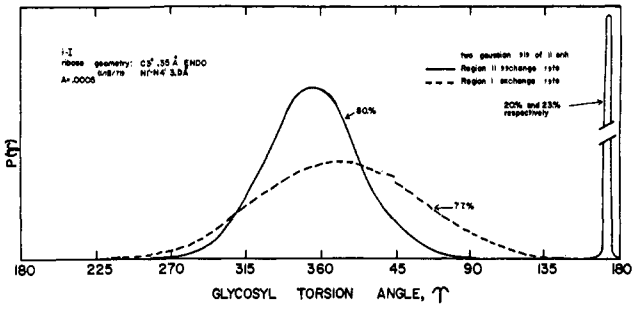

Figure 7. Best fit glycosyl conformation distribution functions for 11 NOE enhancements in i-I in DMSO-d_6. *Cf.* Table III, columns 5 and 7.

$\delta\Upsilon_2$, are probably best regarded as qualitative indicators of the widths of the actual distribution functions (Figure 7). We conclude therefore that i-I exists predominantly ($\approx$80%) in the syn conformation centered at $\Upsilon \approx 355°$, but with about 20% of the population in an anti conformation centered at $\Upsilon \approx 166°$.

A more limited, and thus perhaps a more typical, set of NOE data is available on 2′,3′-isopropylideneuridine (i-U). The NOE enhancements for i-U are shown as a function of Υ in Figures 8 and 9. The results are similar to those for i-I (Figures 4–6) except for $f_6(5)$ (Figure 8). Since the distance between H-5 and H-6 does not change with Υ, one might not expect $f_6(5)$ to be so sensitive to conformation. This strong dependence on Υ is not a three-spin effect, but is due simply to the varying contributions of the ribose protons to the total relaxation rate (R_6) of H-6 (*cf.* eq 2–4). The minimum NOE corresponds to the very close approach of H-2′ to H-6 at $\Upsilon \approx 100°$.

Table V presents the results of the i-U data analysis. As before, the results do not depend strongly on ribose geometry, provided either a planar or C-3′ endo ribose is used, or on the rate of internal rotation. $A = 0.0$ works as well or better than any other value. The final-fit standard deviations are, however, not as good as for i-I. Note, however, that nearly all of the error is in $f_8(3')$; the other four enhancements have a σ of about 0.02. However, referring to Table IV, column 3, we found for the single-Gaussian fit on i-I that $f_8(3')$ did not fit nearly as well as the other enhancements; only a two-Gaussian fit (column 1, Table IV) could improve the calculated value. For i-U, we interpret our inability to fit $f_6(3')$ (corresponding to $f_8(3')$ in i-I) as indicating a small contribution from anti conformations and conclude that the major conformation for i-U is also syn.

Table V. NOE Results for i-U

Obsd {satd}	Av exptl $f_i(j)$	$\Delta f = f_{exptl} - f_{calcd}$: Geometry IIIC,[a] region II, $A = 0.0$	Geometry IIIC, region I, $A = 0.0$	Geometry II,[b] region II, $A = 0.0$
6 {1′}	0.20	0.01	0.03	0.01
6 {2′}	0.10	0.02	0.01	0.02
6 {3′}	0.06	0.08	0.07	0.08
6 {5′}	0	0	0	0
6 {5}	0.23	−0.01	−0.01	0
Υ, deg		17	21	17
δΥ, deg		64	97	62
σ		0.04	0.04	0.04

[a] Geometry IIIC has a ribose identical with that of IIIA except for the O-4′–C-1′–N-1 vertex, which is 110°, as in the X-ray of uridine monophosphate.[28] The glycosyl bond and uracil dimensions were also taken from ref 28. [b] Isopropylidene methyls included.

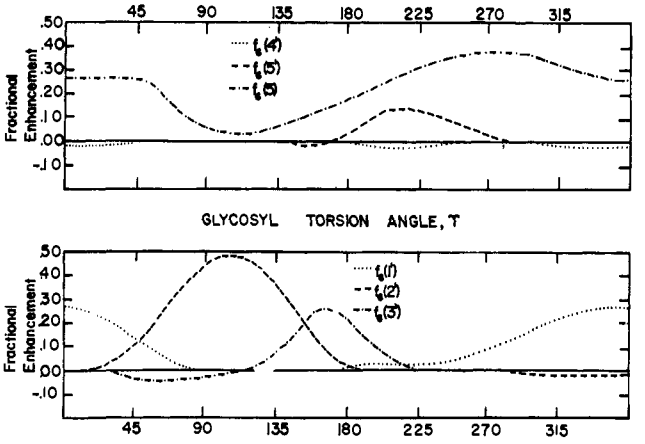

Figure 8. Plots of calculated intramolecular NOE's for i-U *vs.* glycosyl torsion angle; $A = 0.0005$, geometry IIIC.

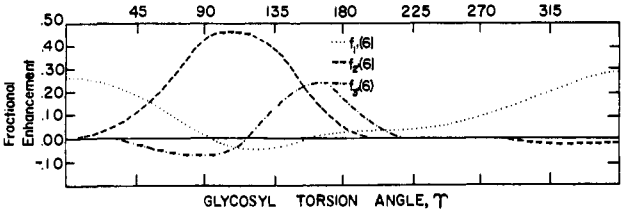

Figure 9. Plots of calculated intramolecular NOE's (see caption of Figure 8).

Figure 10 shows the glycosyl torsion angle distribution function for i-U. As usual, the distribution is broader if region I equations (slow region) are used for the calculation than if region II equations are used. If enough experimental NOE's had been available to perform a two-Gaussian fit on i-U, we would expect that the syn distribution would be narrower and that a small distribution in the anti region would be evident.

Discussion

Extensive comparison of the above results with those obtained by other methods is difficult because few empirical data are available for the compounds and conditions used here. However, a few comparisons are possible. Nucleoside conformational assignments have been made on the basis of CD data.[30] If purine and pyrimidine nucleoside ellipticities in DMSO vary with glycosyl torsion angle in the same way those measured in water apparently do, then according to postulated ellipticity correlations in water[31] i-U in DMSO[19] should have a glycosyl conformation in the region $\Upsilon = 60–200°$. The NOE data herein are not consistent with this expectation. Further qualitative discrepancies between NOE and some published CD interpretations in the pyrimidine nucleoside series have been discussed.

The apparent insensitivity of purine nucleoside B_{2u} ellipticity to the glycosyl torsion angle in the ranges

(30) See ref 8, pp 102 ff.
(31) D. W. Miles, M. J. Robins, R. K. Robins, M. W. Winkley, and H. Eyring, *J. Amer. Chem. Soc.*, 91, 831 (1969).

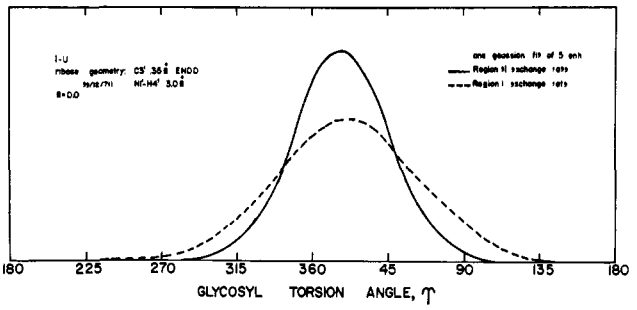

Figure 10. Best fit glycosyl conformation distribution functions for five enhancements in i-U in DMSO-d_6 (see Table IV).

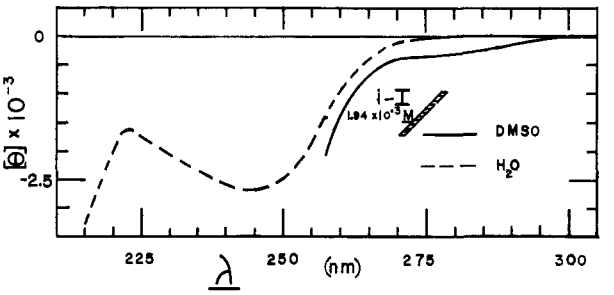

Figure 11. Circular dichroism spectra of i-I at 25°.

Υ = 80–160° and 280–360°[32] makes precise CD–NOE comparisons in these regions tenuous at this point. However, according to the nomograph of ref 32, the sign of ellipticity of adenosine-like nucleosides having a glycosyl torsion angle in the range Υ = 80–160° is expected to be negative, while for Υ = 280–360° it is expected to be positive. The measured ellipticity of i-I in DMSO and in water (Figure 11) is negative in a situation where a glycosyl conformation of Υ = 315 to 45° is known from the NOE analysis herein to be strongly favored.

Chemical shift and coupling constant data from i-I as a function of temperature neither contradict nor corroborate the quantitative NOE results. From the very small changes in $J_{1',2'}$, $J_{2',3'}$, and $J_{3',4'}$ from 30 to 75° (Table VI), one deduces that at 30° the ribosyl moiety is either undergoing rapid interconversion to its various conformationally isomeric states or it is deep in the energy well of one conformation. Specific changes in the anisotropy effects of the aromatic nucleobase on the ribose chemical shifts are expected if the glycosyl rotamer population changes significantly. From the lack of variation of specific ribose chemical shifts with temperature (Table VI), we conclude that the glycosyl conformational distribution is also insensitive to temperature in the range studied.

Table VI. Temperature Effects on Chemical Shifts[a] and Ribose Spin Coupling Constants[b] for i-I[c] in DMSO-d_6

Temp, °C	Proton H-8	H-2	H-1′	H-2′	H-3′	H-4′	H-5′s
30	8.30	8.08	6.10	5.26	4.94	4.22	3.56
45	8.30	8.08	6.10	5.27	4.94	4.22	3.56
75	8.24	8.02	6.10	5.27	4.94	4.24	3.58
	$J_{1'2'}$		$J_{2'3'}$			$J_{3'4'}$	
	2.9 Hz		6.2 Hz			2.6 Hz	

[a] Expressed as δ, parts per million from TMS. *Cf.* Experimental Section. [b] Measured at 100 MHz. *J*'s were invariant, ±0.5 Hz from 30 to 75°. [c] 0.25 *M* plus 1.8% v/v *tert*-butyl-d_1 alcohol.

On the other hand, variable-temperature nmr experiments on i-U provide interesting ribose proton chemical shift correlations. One expects the width of the glycosyl conformer distribution to increase with temperature. If a C-2 oxygen anisotropy effect is operative,[16] the simultaneous increase of $\delta_{H\text{-}2'}$ and decrease of $\delta_{H\text{-}1'}$, $\delta_{H\text{-}3'}$, $\delta_{H\text{-}5'}$ with an increase of temperature (Table VII) from 30 to 130° are consistent with a depopulation of the syn range and a spreading of the population to the wings of the distribution. The

Table VII. Temperature Effects on Chemical Shifts[a] and a Ribose Spin Coupling Constant for i-U[b] in DMSO-d_6

Temp, °C	Proton H-6	H-1′	H-5	H-2′	H-3′	H-4′	H-5′s	$J_{1'2'}$, Hz
30	7.85	5.88	5.66	5.00	4.72	4.08	3.58	2.6
80	7.80	5.88	5.63	*c*	*c*	4.10	3.60	2.5
100	7.76	5.88	5.61	*c*	*c*	4.11	3.62	2.3
130	7.75	5.88	5.61	4.91	4.78	4.12	3.64	2.2

[a] Expressed as δ, parts per million from TMS. [b] 0.25 *M* in pure DMSO-d_6. Degassed and sealed under 10^{-5} Torr pressure. [c] δ is difficult to measure in this temperature range because H-2′ and H-3′ form a complex multiplet at 60 MHz, the frequency at which these experiments were done.

i-U ribose spin coupling constants vary insignificantly with temperature (Table VII). Because virtually no nmr-based nucleoside conformational analysis in DMSO have been reported and because none have been performed on the isopropylidene derivatives, further comparison of the conformational deductions stated here with the many other nucleoside and nucleotide nmr analyses published in the last several years does not appear warranted.

However, the quantitative NOE results can be related to theoretical considerations of nucleoside conformation (see Figures 12 and 13). The simplest predictive procedure that has been employed in this field is that of tabulating the van der Waals contacts of hard-sphere atoms in the model molecule as a function of the glycosyl torsion angle for different ribose geometries. Steric analyses of this type have been performed by Haschemeyer and Rich[9] and by Lakshminarayanan and Sasisekharan.[10] The former authors concluded that the ribosyl conformation was of some importance in determining allowed glycosyl conformations, whereas the latter group concluded that this was not significant. Lakshminarayanan and Sasisekharan,[10] allowing only normal contacts of the nucleobase with the C-3′ endo sugar, concluded that for purine nucleosides Υ can equal 180–230°. When rare contacts were allowed, torsion angles in the syn range (Υ = 20–40°) were also found to be acceptable. For the pyrimidine nucleosides, using both the normal and rare contacts the computed conformational distribution was in the anti range (Υ ≅ 180–240°).

Jordan and Pullman[14] found energy minima for adenosine-type purine nucleosides at Υ = 100 through

(32) D. W. Miles, S. J. Hahn, R. K. Robins, M. J. Robins, and H. Eyring, *J. Phys. Chem.*, 72, 1483 (1968).

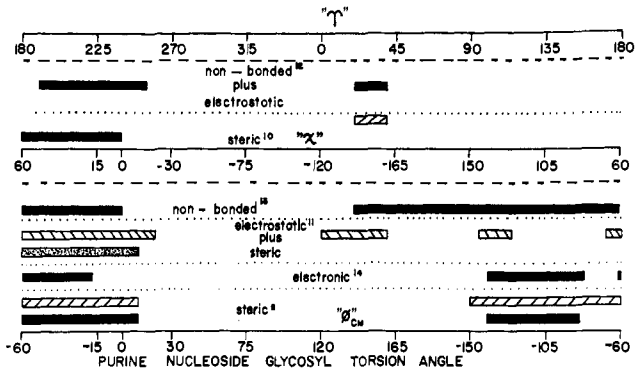

Figure 12. Summary of theoretical predictions of glycosyl torsion angle for purine and pyrimidine C-3′ endo ribose nucleosides. Shaded areas denote allowed or preferred ranges: ( ) in steric calculations denotes "only normal van der Waals contacts allowed;" ( ) "normal and rare van der Waals contacts allowed;" ( ) −70°; ( ) +90°.

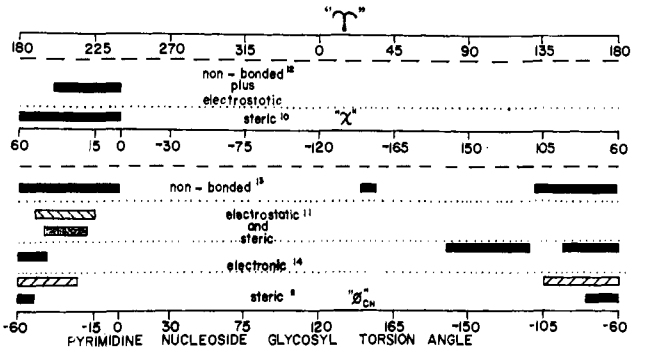

Figure 13. See caption and key to Figure 12.

220° and discerned a small energy difference between the syn and anti forms. Their calculations were of the total electronic energy for a representative set of glycosyl conformations. Minima at Υ = 80 through 200° were found for the uridine-type (as opposed to cytidine) pyrimidine nucleosides. The Tinoco group,[11] combining steric and molecular orbital calculations, derived allowed adenosine Υ values of 180 to 250° at −70° and the additional range of Υ = 0 to 40° at +90°. These authors concluded that for adenosine-type purine nucleosides (as opposed to guanosine type) the total steric and electronic energy difference between the syn and anti conformers is 1–2 kcal/mol and that reasonable changes in ribose geometry could lead to syn as the most stable conformation for adenosine type nucleosides. The steric electronic calculations allow only a single narrow range of conformations for the pyrimidine nucleosides between Υ = 200 and 220° for the temperature range −70 to +90° because the total energy gap between the syn and anti conformers of the pyrimidine nucleosides is 5–7 kcal/mol. Lakshminarayanan and Sasisekharan,[12] combining nonbonded interactions and single atom Coulombic interactions in potential energy calculations, concluded that C-3′ endo sugar geometry (the important geometry for the present considerations) is correlated with probable purine glycosyl torsion angles of Υ = 190–255° and 20–40° and a probable pyrimidine torsion angle of Υ = 200–240°. Wilson and Rahman[13] made similar computations including only nonbonded interaction potentials and found (for the 3′-endo sugar case) that low-energy glycosyl rotamers are probable at Υ = 190–240° and 20–140° for the purines and Υ = 130–240° for the pyrimidines. A very narrow and relatively high energy distribution is probable at Υ = 25–35° for the pyrimidines. In general, both groups conclude that low-energy glycosyl conformations in both the syn and the anti range occur in the C-3′ endo purine nucleosides, but the anti range is clearly preferred for the C-3′ endo pyrimidine nucleoside.

The present NOE data contradict the above theoretical treatments with respect both to the normally expected relative distributions of the C-3′ endo purine nucleoside glycosyl rotamers and to the expected single preferrred distribution of the C-3′ endo pyrimidine nucleosides. Solvent effects and intermolecular association may be responsible for this disparity.

Solvent effects on nucleoside conformation would be significant because of the interaction between the net sugar and heterocycle dipoles. In simpler systems, *e.g.*, 1,2-dibromocyclohexanes,[33] the conformer with the largest total net dipole is stabilized by polar solvents. Unfortunately, although charge density calculations have been made on representative nucleoside systems[14] and although dipole moment calculations have been made on guanine, uracil, adenine, and cytosine,[34] no published net nucleoside dipole moment calculations as a function of torsion angle are available. It is, therefore, not possible to say which of the two extreme glycosyl conformations (syn or anti) would be the more polar.

Although guanosine associates appreciably in DMSO,[35] the nucleosides of this study probably do not. Newmark and Cantor[35] have shown that cytidine does not associate in DMSO, and Hart and Davis[19] have shown that uridine, isopropylideneuridine, cytidine, and isopropylidenecytidine do not self-associate appreciably in polar solvents. No studies are available on the self-association of hypoxanthine nucleosides. In any event intermolecular association can be discounted as a determinant of conformation in the present systems not only because the extent of base pairing is minimal but also because the possible structures of the hydrogen bonded complexes is such (*cf.* ref 35) that no significant perturbation of the glycosyl or ribose conformation is expected.

In summary, it is likely that some undefined solvent effect determines the nucleoside glycosyl torsion angle in solution.

Conclusion

The utility of the nuclear Overhauser effect for the determination of molecular conformation in solution has been demonstrated. The experiment is suited to probing both short-range proton–proton resonance interactions, as in the present case, and heteronuclear resonance interactions (*e.g.*, $^{1}H-^{13}C$, $^{1}H-^{15}N$, $^{1}H-^{31}P$, $^{15}N-^{31}P$, etc.). The method is therefore potentially

(33) P. Bender, D. L. Flowers, and H. L. Goering, *J. Amer. Chem. Soc.*, 77, 3463 (1955), and references therein.
(34) B. Pullman in "Molecular Orbital Studies in Chemical Pharmacology," L. B. Kier, Ed., Springer-Verlag, New York, N. Y., 1970.
(35) R. A. Newmark and C. R. Cantor, *J. Amer. Chem. Soc.*, **90**, 5010 (1968).

useful for structural and conformational analyses of a variety of chemical systems.

The weaknesses of this method are the stringent requirements on the nmr chemical shifts of the nuclei studied and the difficulty in obtaining accurate and reproducible intensity measurements in nmr. These can be overcome to some extent by the improved spectrometers now available; for example, use of superconducting magnets will extend the range of application by increasing the chemical shifts, and heteronuclear spin lock combined with signal averaging will contribute to more facile and accurate intensity measurements. The advantage of the technique lies in the simplicity of the theory and the direct connection between experimentally measured quantities and molecular geometry; no calibration or empirical relationships are required. In addition, the sixth power dependence of the measured quantities on the geometrical parameters causes the relatively inaccurate measurements and approximations to have a minimal effect on the accuracy of the technique.

The resolution of the technique is difficult to define since only limited experience is available. Since the NOE depends on *relative* internuclear distances, the resolution will actually vary from case to case. It would appear from the examples reported here that a resolution of 0.1 Å is not an unreasonable expectation. This accuracy is still limited by experimental error so that improvements in experimental technique are well worthwhile.

Other solution structure probes, such as fluorescence, electron spin labeling, and circular dichroism, have resolving powers on the order of molecular dimensions and therefore are more useful for the analysis of macromolecular shape. Indeed, the value of quantitative proton NOE's is mitigated in species of molecular weight greater than about 400 because of line-broadening and the probable occurrence of overlapping resonances.

Acknowledgments. Joseph H. Noggle and Roger E. Schirmer were supported by the National Science Foundation (Grant No. GP-15068). Phillip A. Hart and Jeffrey P. Davis received support from the Wisconsin Alumni Research Foundation and from a General Research Support Grant of the National Institutes of Health. The University of Wisconsin Chemistry Department HA-100 spectrometer facility was provided by funds from the National Science Foundation (Grant No. GP-52-10). Computer calculations were carried out on a Univac 1108 Time Sharing Executive Computer maintained by the University of Wisconsin Computing Center.

Appendix I

In computing enhancements using eq 7 and 12, it was assumed that $\rho_j(\Upsilon)^*$ was a constant independent of j and Υ, and it was further assumed that $\tau_C(ij)$ was the same for all i and j. These assumptions allow the $\rho_{ij}(\Upsilon)$ to be replaced by $r_{ij}(\Upsilon)^{-6}$ in eq 7 and 12 when $\rho_j(\Upsilon)^*$ is replaced by

$$A = \rho^*/\gamma_j{}^4\hbar^2\tau_C$$

A has been treated as an adjustable parameter in the calculations reported here, and has further been assumed to be the same for all spins. In properly prepared samples (well degassed, sealed, low concentration of ^1H or ^{19}F nuclei, no paramagnetic impurities), the values of the A's will be small and the NOE will not be too sensitive to their exact value.

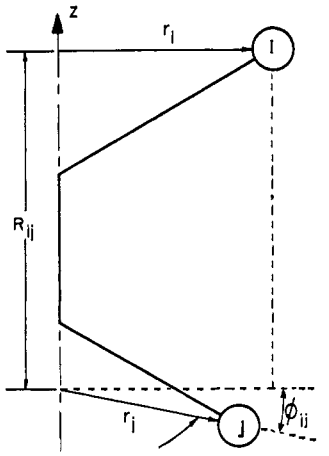

Figure 14. Definition of geometrical parameters for computation of relaxation parameters for a single internal rotation using eq A1. Z is the axis about which the internal rotation occurs (in this instance, the glycosyl bond); r_i and r_j are the perpendicular distances between the Z axis and spins i and j, respectively; R_{ij} is the difference in the Z coordinates of spins i and j; ϕ_{ij} is the angle between the vectors $\mathbf{r}_i$ and $\mathbf{r}_j$ when the torsion angle is zero (in this instance, $\Upsilon = 0$).

Calculations of Enhancements in Region I. The values of $r_{ij}(\Upsilon)^{-6}$ required to calculate the enhancements were computed using the relation

$$r_{ij}(\Upsilon)^{-6} = [Z_{ij}{}^2 + r_i{}^2 + r_j{}^2 - 2r_ir_j \cos(\phi_{ij} + \Upsilon)]^{-3} \quad \text{(A1)}$$

In this equation, Υ is the torsion angle about the glycosyl bond and the other geometric parameters are as defined in Figure 14.

The calculation of $f_d(s)$ was begun by constructing a table of $f_i(j,\Upsilon)$ as a function of τ using an iterative technique for the solution of eq 5. The iterative procedure consisted of the following steps.

(1) Estimate all $f_m(n,i)$ using

$$f_m(n,\Upsilon) \approx \frac{\rho_{mn}(\Upsilon)}{R_m(\Upsilon)} = \frac{r_{mn}(\Upsilon)^{-6}}{A + \sum_j r_{mj}(\Upsilon)^{-6}}$$

where the $r_{mn}(\Upsilon)^{-6}$ are calculated using eq A1 and A is given some suitable value.

(2) Substitute the estimated values of $f_m(n,\Upsilon)$ back into eq 5 to obtain new estimates for all the $f_m(n,\Upsilon)$.

(3) Repeat step 2 until all the $f_m(n,\Upsilon)$ on iteration N are within a preset limit of their value on iteration $(N - 1)$. Convergence is generally obtained in just a few iterations.

The final step in the calculation of the $f_d(s)$ that would result from a distribution $P(\Upsilon)$ was to perform a Simpson's rule integration[36] of eq 7 using $P(\Upsilon)$ and the tabulated values of $f_d(s,\Upsilon)$. When the problem was to determine the distribution that best fit a set of experimental enhancements, an algebraic form for the distribution function was selected and a least-squares fit of the parameters in the function to the data was performed. The least-squares fit was done using the

(36) B. Carnahan, H. A. Luther, and J. O. Wilkes, "Applied Numerical Methods," Wiley, New York, N. Y., 1969, Chapter 2.

University of Wisconsin Computing Center library subroutine UWHAUS which employs Marquardt's algorithm[37] to accomplish the fitting. The functional form was generally that of the sum of squares of two Gaussians so that there were five variable parameters to be determined.

Calculation of Enhancements in Region II. The calculation of $f_d(s)$ in the intermediate rate range began with the calculation of the average values of $r_{ij}(\Upsilon)^{-6}$ by a Simpson's rule integration of eq 13. The values of $\langle r_{ij}^{-6} \rangle$ are then used in place of the $\langle \rho_{ij} \rangle$ to solve eq 12 for $f_i(j)$ using the iterative procedure described above. The least-squares fits were accomplished in the same manner for region I and region II calculations.

Appendix II

Primary Geometries. Unsubstituted cyclopentanes and pentaheterocycles can exist in several formally distinct, low-energy conformational states in addition to the strained planar depiction.[38,39] Conceptually[40] these states are permutations around the ring of two basic geometric forms: the envelope, of C_s symmetry, in which one atom is out of the plane of the other four, and the half-chair, of C_2 symmetry, in which two atoms deviate from the plane of the other three, one above and one below.

Of the three parameters, the sugar ring puckering, the C-4′, C-5′ torsion angle, and the glycosyl torsion angle, that uniquely specify a nucleoside conformation, the glycosyl torsion angle is the strongest determinant of conformation dependent physical properties (*e.g.*, dipole moment, optical activity, etc.). First principles require that the C-4′ hydroxymethylene (C-5′, O-5′) substituent and the nucleobase be pseudoequatorial, thus creating a C_s form of tetrahydrofuran (with the ring oxygen puckered endo). In working with models, we express the relative disposition of these two substituents in terms of the corresponding H-1′, H-4′ distance. For a 2′,3′-dideoxy-β-ribonucleoside such a puckered conformation (O-1′ 0.4 Å endo) would relieve the intrinsic strain of the planar system. However, the ribose cis glycol acetonide favors a staggering of the oxygen atoms by analogy with the 2,2′-dimethyl-1,3-dioxolane system.[41] C-3′ 0.35 Å endo and an H-1′, H-4′ distance of about 3.0 Å (geometry III^A) satisfy the requirements of the pseudoequatorial bulky substituents and of the skewed cis vicinal oxygens and are also consistent with the observed ribose coupling constants (Table VI). In comparison with others tested (see Table II) this geometry gives some of the best conformational fits[42] for NOE data on nucleoside 2′,3′-isopropylidene derivatives including the two discussed in this paper.

(37) D. W. Marquardt, *J. Soc. Ind. Appl. Math.*, **2**, 421 (1963).
(38) K. Pitzer and W. Donath, *J. Amer. Chem. Soc.*, **81**, 3213 (1959).
(39) R. Lemieux in "Molecular Rearrangements," Vol. 2, P. deMayo, Ed., Wiley-Interscience, New York, N. Y., 1964.
(40) L. Hall, P. Steiner, and C. Pedersen, *Can. J. Chem.*, **48**, 1155 (1970), have suggested a very useful convention for denoting ribose geometry. For example, C-3′ 0.4 Å endo is ^{3}V; C-3′ 0.4 Å exo is V$_3$′; C-3′ 0.2 Å endo, C-4′ 0.2 Å exo is ^{3}′T$_4$′; etc.
(41) R. Lemieux, J. Stevens, R. Fraser, *ibid.*, **40**, 1955 (1962).
(42) J. P. Davis, unpublished experiments.

Halogen Substituent Effects on the Circular Dichroism of Pyrimidine Nucleosides. Nuclear Overhauser Effect and Circular Dichroism Correlations

Phillip A. Hart* and Jeffrey P. Davis

Contribution from the School of Pharmacy, University of Wisconsin, Madison, Wisconsin 53706. *Received July 9, 1971*

Abstract: On the basis of quantitative intramolecular nuclear Overhauser effects, 5-fluoro-, 5-chloro-, 5-bromo-, and 5-iodouridine are shown to be conformationally homogeneous in deuterium oxide and deuterated dimethyl sulfoxide (DMSO-d_6) or in mixtures of the two solvents. The ultraviolet spectra of the series vary with the halogen substituent transition moments, and the corresponding circular dichroism spectra evince a large influence of the 5-halogen substituent on the B_{2u} Cotton effect. Because of the conformational homogeneity of the series, differences in the circular dichroism spectra of the 5-halouridines in these solvents are attributed to direct electronic effects of the substituents.

The glycosyl torsion angle, Υ, of the pyrimidine ribonucleosides (see ref 1 for definition) is an important parameter in studies of RNA and t-RNA solution conformation.

Unusual pyrimidine nucleotide units characterized by rare aglycone substitution patterns appear in t-RNA's in particular[2] (*e.g.*, 4-thiouridine, 2-thiouridine, ψ-uridine). Some of these manifest the *syn*-glycosyl conformation in the solid state.[3] Knowledge of nucleobase substituent effects on nucleoside conformation in solution (particularly glycosyl conformation) is therefore of value.

Whereas pyrimidine nucleosides have generally been thought to assume the anti conformation in solution (**1**, Figure 1), we have unequivocally established the glycosyl conformation of 2′,3′-isopropylideneuridine in DMSO

(1) R. E. Schirmer, J. P. Davis, J. H. Noggle, and P. A. Hart, *J. Amer. Chem. Soc.*, **94**, 2561 (1972).
(2) K. Miura, *Progr. Nucl. Acid Res. Mol. Biol.*, **5**, 39 (1967).
(3) W. Saenger and K. Scheit, *Angew. Chem., Int. Ed. Engl.*, **8**, 139 (1969).